| | |
|---|---|
| **Publication details:** | Susanne Heinzel, Tran Binh Giang, Andrey Kan, Julia M Marchingo, Bryan K Lye , Lynn M Corcoran, Philip D Hodgkin. A Myc-dependent division timer complements a cell-death timer to regulate T cell and B cell responses. Nature Immunology 2017 Jan;18(1):96-103. |
| **Final authenticated version Is available online at:** | https//doi.org.10.1038/ni.3598 |

# A Myc-dependent division timer complements a cell death timer to regulate T and B cell responses

Susanne Heinzel[1,2], Tran Binh (Andrew) Giang [1,2], Andrey Kan[1,2], Julia M Marchingo[1,2,4], Bryan K Lye[1 ,2], Lynn M Corcoran[3,2] and Philip D Hodgkin[1,2]*

[1] Division of Immunology, The Walter and Eliza Hall Institute of Medical Research, Parkville, VIC, Australia.

[2] Department of Medical Biology, The University of Melbourne, Parkville, VIC, Australia.

[3] Division of Molecular Immunology, The Walter and Eliza Hall Institute of Medical Research, Parkville, VIC, Australia.

[4] Present address: Division of Cell Signalling and Immunology, School of Life Sciences, The University of Dundee, Dundee, Scotland, UK.

* To whom correspondence should be addressed. Email: hodgkin@wehi.edu.au

**Abstract**:

T and B lymphocytes integrate activating signals to control the size of their proliferative response. Here we report that control is achieved by timed changes in the production rate of cell cycle regulating proto-oncogene Myc with division cessation occurring when Myc levels fall below a critical threshold. The changing pattern of Myc level is not affected by cell division identifying the regulating mechanism as a cell-intrinsic, heritable temporal controller. Overexpressing Myc in stimulated T and B cells does not sustain cell proliferation indefinitely as a separate time to die mechanism, also heritable, is programmed upon activation leading to eventual cell loss. Together the two competing cell intrinsic timed fates create the canonical T

and B cell immune response pattern of rapid growth followed by loss of most cells. Further, small changes in these timed processes by regulatory signals, or by oncogenic transformation, synergize to significantly enhance cell numbers over time.

**Introduction:**

T and B lymphocytes integrate activating signals to trigger a controlled proliferation burst. The magnitude of this burst, and hence the strength of the early immune response, is subject to intense regulation by numerous signals[1, 2, 3]. Many of these signals alter kinetic features of proliferation and survival simultaneously making it difficult to separate effects on one or the other cellular process. These difficulties are a setback for development of multi-scale immune models that can accommodate and account for molecular, cellular and whole system behavior. Given this difficulty quantitative analytical tools are being developed to help separate each influence with the dual goal of informing the search for suitable molecular mechanisms and guiding the development of integrative models. Here we apply quantitative methods to clarify the molecular and cellular modes of control of proliferation and death following stimulation of T and B lymphocytes.

It was shown previously that the total number of divisions undergone before returning to quiescence (termed the cell's division destiny, DD)[1, 4, 5], is regulated by numerous costimulatory and cytokine signals[1, 5] and the net effect of combining inputs on the final division number is accurately predicted with a simple rule of addition[1]. The quantitative precision of this signal integration suggested the underlying molecular mechanism might now be tractable. As an initial hypothesis we proposed a molecular mechanism where a downstream signaling product, motivating cell division, accumulates in direct proportion to activating inputs and is subsequently lost to end the division burst[5].

Here we tested this hypothesis by asking, initially, if, the mitotic regulator Myc, served as the division-motivating factor. Myc was a candidate for the primary controller due to its well established role in transitioning cells from growth to quiescence in numerous cell types including normal stimulated B and T lymphocytes[6] and hematopoietic and embryonic stem cells[7]. Myc is a key component controlling the metabolic changes to glycolysis in T and B cells after antigenic signaling[8, 9, 10]. In lymphocytes Myc expression is induced through a number of different signaling pathways with many of these being directly downstream of T and B cell activating and costimulatory receptors[6, 11]. We also anticipated that the putative factor would be an oncogene if deregulated given its role in cell division. By this criteria Myc was again a strong candidate. Deregulated Myc plays an important role in cancer progression in many human tumors[12, 13, 14]. Furthermore, Eμ-Myc transgenic (Tg) mice, which over-express Myc in B lymphoid cells rapidly succumb (mean survival ~120 days) to clonal B cell lymphoma[15].

Our results confirm the identity of Myc as the putative regulator of DD, but not as the division counter we initially proposed. Rather we report that Myc serves to drive a division-independent temporal control mechanism. We also show that this mechanism is integrated with an independent control mechanism for cell death and together they generate the typical patterning of the adaptive immune response.

## Results

### Myc drives a division destiny timer.

**Fig. 1** illustrates two possible modes of controlling the extent of a cell division burst by accumulation and loss of a division promoting factor: A division counter (**Fig. 1a**); or a timer **(Fig. 1b**). To establish a potential role for Myc in regulating the number of generations in either

manner we first determined Myc expression kinetics after activation of B and T cells. Naive B cells from C57BL/6 mice (wild-type) were stimulated with the Toll-like receptor 9 (TLR9) ligand CpG (**Fig. 1c-f**). As T cell regulation is complicated by the simultaneous changes in cell survival and rapid death we used OT-I T cell receptor Tg $CD8^+$ T cells that lacked the pro-apoptotic molecule Bim (*Bcl2l11*) (referred to hereafter as OT-I/*Bcl2l11*$^{-/-}$). It was shown previously that the elimination of Bim markedly delays time to die but does not affect division destiny in T cells[1] or B cells[5]. OT-I/*Bcl2l11*$^{-/-}$ were stimulated with their cognate peptide antigen SIINFEKL (N4) and anti-CD28 antibody **(Fig. 1g-i**).

As previously reported, both cell types followed a programmed response, triggering an initial proliferative burst before returning to quiescence and eventually dying[1, 5] (**Fig. 1c-e,g,h**). Myc protein level in these cells initially rises and then progressively declines over time, returning to background levels at times coinciding with division cessation (**Fig. 1e,f,h,i; Supplementary Fig. 1)**. We measured Myc protein within each generation of cells (as determined by division tracking dye CellTrace Violet (CTV)) to test whether the amount of Myc was diminishing by division (as proposed in **Fig. 1a**). For both cell types, Myc expression changed over time but was stable throughout generations at any given time point **(Fig. 1j-o**). Thus, if Myc is the division-motivating factor we hypothesize, this pattern of Myc expression is not consistent with the 'counter' machinery (**Fig. 1a**) but would identify the molecular machinery as a division-independent temporal controller (**Fig. 1b**).

**Temporal control of DD is independent of death**

To explore a causative link between Myc and DD we manipulated Myc levels with a Myc-expressing retrovirus in CpG activated B cells. Control (empty vector) transduced cells divided before stopping at an average of 4 generations (**Fig. 2a,b**). Division cessation occurred around 75 h, shortly before cell numbers declined due to cell death. As expected, forced expression of

Myc increased the number of generations the cells underwent resulting in greatly enhanced cell numbers (**Fig. 2a-c and Supplementary Fig. 2a**). Myc overexpression had little effect on the division rate, with a similar mean division number (MDN) observed in both cultures until the control infected cells stopped dividing (**Fig. 2b**). Of note, in these cultures population growth was still limited due to cell death (at ~90 h), despite the continued expression of Myc in the transduced B cells (**Fig. 2a-c, Supplementary Fig. 2a**). This suggested temporal control of death was induced upon activation, and continued to operate independently of whether cells were dividing or had returned to the quiescent state. If correct, population numbers should continue to increase for Myc expressing cells if their survival could be maintained. We confirmed this prediction by using B cells from mice overexpressing the survival factor Bcl-2 (Bcl-2-Tg)[16]. Lymphocytes from these mice have an extended, but not unlimited, life span[17]. Bcl-2-Tg B cells infected with the control vector underwent the same number of divisions as cells from wild type mice but survived in culture for longer, as expected[5] (**Fig. 2d,e** and **Supplementary Fig. 2b**). In contrast Myc overexpressing cells continued to divide and a decline in cell numbers was only observed when they reached a new, much later death time (here ~ 250 h) (**Fig. 2d,e**). We further confirmed the role of Myc as the regulator of DD using two transgenic systems for overexpressing Myc in B and T cells (**Supplementary Fig. 2e-h**). As expected, cells from the transgenic mice exhibited increased DD when stimulated. Thus, Myc clearly drives division progression, whereas an independent timed process controls cell death, thereby serving as a safeguard against unlimited growth.

**Signal integration determines Myc level and DD time**

Having identified Myc as a driver of DD, and that the regulatory mechanism followed temporal not division-based control, we next tested whether the amount of Myc would serve as a quantitative integrator of signals received. OT-I/*Bcl2l11*$^{-/-}$ CD8$^{+}$ T cells stimulated with N4

and varying concentrations of anti-CD28 antibody showed a dose-dependent increase in total cell numbers (**Fig. 3a**) and in $DD^1$ (**Fig. 3b**). At 24 h, before cells entered their first division, Myc protein reached higher amounts with increased stimulation and then declined at an approximately exponential rate (**Fig. 3c**). Thus at the time of division cessation in weakly stimulated cells (dashed line in **Fig. 3b** and **c**) the amount of Myc protein was close to background whereas strongly stimulated cells still expressed high amounts of Myc at that time point.

To investigate whether the accumulation of Myc also applied to combinations of signals, we examined the impact of anti-CD28 antibody and IL-2 alone or together on T cells. Both Myc amounts at 23 h (**Fig. 3d**) and DD (**Fig. 3e,f**) increased with the addition of IL-2 or anti-CD28 antibody to N4 stimulated OT-I/*Bcl2l11*$^{-/-}$ $CD8^+$ T cells and increased even further when both stimuli were present (**Fig. 3d-f)**. When Myc protein measured at 23 h was plotted against DD, a strong correlation between the strength of the activating signal, Myc amounts and DD was observed in $CD8^+$ T cells (**Fig. 3g**) as well as in B cells (**Fig. 3h**). These findings suggest that the change in net signal strength arising from multiple inputs is integrated through the amount of Myc protein that in turn determines the DD of the population.

**Myc degradation rate does not account for the timed loss.**

These results raise the question of how the Myc-dependent division timer operates and is retained through multiple division rounds. A detailed time course of OT-I/*Bcl2l11*$^{-/-}$ $CD8^+$ T cells stimulated with N4 peptide and increasing concentrations of anti-CD28 antibody revealed that both the amplitude and the time taken to reach that level before a progressive loss was observed were dose-dependent on the stimulation strength (**Fig. 4a** and **Supplementary Fig. 3a**). The rate of loss, once begun, conformed approximately to an exponential curve. Stronger

stimulation increased DD time resulting in more divisions (**Fig. 4b** and **Supplementary Fig 3b**). Linear regression (with the same slope forced) of the log transformed data of the decay phase revealed that Myc protein amounts were approximately equal at the times when division ceased for each of the five stimulation conditions tested (**Fig. 4c** and **Supplementary Fig. 3c**), identifying a putative 'division threshold level' of Myc. The half-life of Myc protein during the decay phase in these cultures was calculated to be around 7 hours.

A possibility for the loss of Myc over time was an increased protein degradation rate. However the similarity in decay rates observed for the different stimulation conditions implied Myc degradation was constant over time and that a change in the rate of production of Myc was, therefore, the dominant control mechanism. To test this conclusion, we used cycloheximide (CHX) to block new protein synthesis. CHX was added to OT-I/*Bcl2l11*$^{-/-}$ CD8$^{+}$ T cells stimulated with N4 peptide, with or without anti-CD28 antibody or IL-2, at several time points and Myc proteins examined for a further 6 h. As reported in other systems[18], when protein synthesis is blocked the half-life of the Myc protein was around 20 min in all stimulation conditions, and was independent of whether Myc amounts in the CHX-free cultures were continuing to increase (i.e. anti-CD28 antibody and IL-2 cultures at 18 h) or had plateaued (i.e. N4 peptide only at 18 h) (**Fig. 4d** and **Supplementary Table 1**). We found that the half-life of Myc remained relatively stable over time and did not diminish at later time points. Additionally Myc production and degradation rates were similar in cells of different generations at the same time point (**Supplementary Fig. 3d**). Thus, the difference of the half-life of the total amount of Myc of around 7 h observed in the culture compared to the half-life of Myc of 20 min means that the net amounts of Myc observed over time are a result of significant ongoing production. Therefore, as Myc degradation is not affected by stimulation, time or division, we concluded that the loss of Myc protein observed must be a function of changes in production rates over time. Together these data explain how Myc levels can be unaffected by cell division (**Fig. 1j-**

**o**). In contrast to a slow turnover rate that would result in division-based protein dilution (**Fig. 1a**), the rapid turnover of Myc protein means that a dynamic equilibrium, balancing production and degradation, is established. As these rates are inherited with division, equilibrium levels reinstate quickly after cell division. Thus, 'timed' changes reducing the rate of production leading to eventual division cessation (**Fig. 1b**) must be transferred and replicated through cell divisions.

**Induced variation in Myc expression determines DD fate**

Even in a population of genetically and phenotypically comparable cells (such as TCR-Tg T cells or naive B cells isolated from a single mouse) not all cells respond identically and a distribution of the division number in which cells stop dividing is always observed[1, 4, 5] (**Fig. 1c, Fig. 3e)**. We hypothesized that if Myc is the primary driver of a division timer, then DD heterogeneity could be explained by the variation in the levels of Myc induced in each founder cell in response to the stimulus. To test this, we used T cells (**Fig. 5a-c**) and B cells **(Fig 5 d-f**) from a Myc-EGFP fusion protein reporter mouse[19] crossed to OT-I mice (OT-I-Myc-EGFP). The EGFP fluorescence of lymphocytes from the OT-1-Myc-EGFP mice correlates directly with the amount of Myc protein as determined by intracellular staining and flow cytometry **(Supplementary Fig. 4a,b**). T and B cells from the OT-I-Myc-EGFP were stimulated for 24 h with N4 and CD28 antibodies or CpG, respectively, before being sorted according to EGFP expression level **(Fig. 5a,d**) and placed back into culture without further stimulation. The amounts of Myc expressed at 24 h strongly determined the number of times the cells divided **(Fig. 5** and **Supplementary Fig 4c,d**). Also, as expected if Myc controls a division destiny timer, cells expressing lower levels of Myc ceased division sooner as shown by the earlier appearance of small cells (**Supplementary Fig.4 e,f**) a surrogate marker for quiescence[1]. These results confirm the direct quantitative link between Myc expression and DD and identify

variation in Myc expression in individual cells as a major determinant of DD heterogeneity at the population level.

**Slowing division does not alter DD or death times**

Activated T and B cells exhibited a time to die that was unaffected by expression level of Myc (**Fig. 1d,g** and **Fig. 2a**). These results implied DD and death times were independent cellular operations and that the information for when to die was also timed and unaffected by cell division. If correct we predicted that manipulating times to divide with anti-mitotic drugs would not alter the heritable times to DD or to die. We tested this prediction with the immunosuppressive S-phase inhibitor Mycophenolic Acid (MPA). MPA slowed division times in OT-I/*Bcl2l11*$^{-/-}$ T cells in dose dependent manner (**Fig. 6a,b** and **Supplementary Fig. 5**). Measuring the number of cells contributing to the total population at each time after adjusting for cell number expansion in each generation, confirmed the rate of death was identical in all cultures (**Fig 6c,d** and **Supplementary Fig. 5c**). Of note, this observation was not due to the absence of Bim as similar results were observed with wild-type OT-I cells (data not shown). Thus, time to die is subject to temporal control and is unaffected by division, as already noted for DD. We also observed that slowing of division times had little effect on the times to reach DD (**Fig. 6a,b** and **Supplementary Fig. 5a,b**), and, as expected from this result, the levels and rate of loss of Myc protein over time was unchanged (**Supplementary Fig 5d**).

**Small changes in DD and death times amplify cell number**

We recognized that the autonomous program underlying early T and B cell immune responses was suitable for further quantitative investigation as a model. To develop a mathematical model based on heritable timed features (**Fig. 7a-e**) we took the following steps: 1. Myc dependent temporal control over division (**Fig. 7a**) was converted to a cell intrinsic timing

mechanism that first motivated, then restricted, ongoing cell division (**Fig. 7b**); 2. A separate competing timed process leading to death was incorporated for each cell (**Fig. 7c**). This heritable death mechanism was a simpler variant of earlier models that required resetting of death time at each generation[4, 17, 20, 21, 22] . To complete the model, division times for first and subsequent divisions were assigned and each timed parameter represented as a distribution to account for cellular differences (**Fig. 7d**). Combined the successive effects of each additional cell feature: division only; division plus DD; and division, DD and death, fashion the typical patterning of the immune response (**Fig. 7e**). Fitting the model to data above (**Fig. 2**) demonstrated how the markedly enhanced proliferation seen in cells with changes to both Myc and Bcl-2 expression was consistent with the independent effect of each alteration alone. Thus, the longer time for division afforded by forced expression of Myc, and the longer time to die due to expressing Bcl-2, when combined using the model, predicted the 5-log change in cell number observed by experiment (**Fig. 7f**).

This model can further illustrate how regulatory signals that effect changes in both DD and time to die will act in synergy to increase (or decrease) cell numbers. Increasing each parameter by only 20% would translate to a 5-fold increase in cell numbers at the response peak (**Fig. 7g**) and lead to 10-100 fold differences in cell numbers during the contraction phase (**Supplementary Fig. 6a,b**).

## Discussion

The high degree of synchrony in division times displayed by T and B cell siblings[4, 21, 23], and the striking symmetry in DD exhibited by members of clonal families[4, 24] has made it difficult to determine whether cells were ‘counting’ divisions or timing a division burst following activation[5]. Identifying Myc as the regulator of the division burst resolves this question. The division-insensitive pattern of Myc increase and loss allows us to reject the division counting

hypothesis and establish temporal control as the correct mode of operation. Timed cell fate control has been described for other cell types and is a frequent method of organ patterning[25, 26], implying immune cells have adapted a broad, evolutionarily ubiquitous program to control the strength of an immune response. Our results also place Myc at the center of a signal integration mechanism where multiple inputs converge to alter the pattern of production and loss. As a result of this integration the time at which Myc falls below a stimulatory threshold and enforces division cessation is proportional to the strength and number of such inputs. While parsimonious with our data, this mechanism raises an intriguing question: How can timed changes in the amounts of Myc be transmitted faithfully from one cell generation to the next? Our first hypothesis, that a heritable Myc degradation rate would increase with time, proved incorrect. Rather, it was the Myc production rate, and timed changes to that rate, that were passed along and reproduced from generation to generation. This conclusion was confirmed by slowing division rates with MPA. In such cultures Myc amounts, and therefore DD times, were unaffected leading to fewer divisions being completed before the destiny time was reached. These observations imply the epigenetic landscape facilitating Myc transcription is time-unstable, either in some intrinsic manner, or via an upstream timed change in the epigenetic marks providing access to the Myc promoters. We must also postulate that during replication the state of epigenetic marking around these promoters is faithfully replicated, as is the reproduction and replication of any extrinsic timed regulators. A study of epigenetic markings around Myc before and after division, as well as the quantitative changes in Myc regulators in cells and descendants, may help solve this intriguing observation.

Despite Myc's clear role in DD control we were surprised that forced expression within activated cells did not lead to continued and unlimited division. Applying quantitative methods to separate effects on division and survival allowed us to identify the reason. Following

activation cells adopt a designated time to die that is not altered by expression levels of Myc and therefore unaffected by the metabolic state of the cells. As a result T and B cells that had either returned to quiescence, or were forced to divide by Myc expression, underwent apoptosis at a similar designated time. These results indicated that regulation of the times for DD and for death were independent within each cell (i.e. Myc has no direct effect on death) in contrast to other studies[27, 28]. These results also demonstrate that the machinery governing time to die in T and B cells is a second example (i.e. after DD control and Myc regulation) of division-independent temporal control. It is this separate, and independent mechanism that prevents forced expression of Myc to lead to unlimited cell growth. Although we have not, as yet, identified the timing mechanism for death, known regulators of apoptosis, Bim and Bcl-2, operate as modifiers of the overall time. Thus, two oncogenes, Bcl-2 and Myc, known to work in synergy for tumor formation[29, 30, 31], dictate the overall strength of an immune response. The model developed here demonstrated how potent the combined effects of Bcl-2 and Myc could be, with virtual unrestrained growth resulting from a doubling of the median DD and death times usually adopted after activation of these primary cells. Thus, there may be only a small step from healthy immune responses to the somatic changes that could lead to deregulated lymphoid growth and tumorigenesis.

Our data also identify how extrinsic signals, such as cytokines and cell contact delivered modulators, are integrated to regulate proliferation of cells. As for cell transformation, our model has illustrated how the mechanism of control is remarkably sensitive. The enormous amplification of small effects underlying both immune cell control and oncogenic transformation highlights the importance of using quantitative tools to correctly identify and measure cellular effects when examining, for example, genetic changes, immunosuppressive drugs and somatic influences.

**Acknowledgments:** We thank S. Cory for the vav-myc10 mice, P. Bouillet for Bcl-2-Tg, *Bcl2l11*$^{-/-}$ and Eμ-myc mice, M. Hancock and T. Kratina for technical assistance, J. Zhou for help in figure preparation, S. Cory, M. Dowling, K. Duffy and A Strasser for critical review of the manuscript. This work was supported by the National Health and Medical Research Council via Project Grants 1010654 and 1057831, and Program Grant 1054925, and fellowships to PDH and LMC. This work was made possible through Victorian State Government Operational Infrastructure Support and Australian Government NHMRC Independent Research Institutes Infrastructure Support Scheme Grant 361646. JMM was supported by an Australian Postgraduate Award, WEHI Edith Moffat Scholarship and Sydney Parker Smith Postdoctoral Research Fellowship from the Cancer Council of Victoria, BKL was the recipient of a Melbourne International Research Scholarship and a Melbourne International Fee Remission Scholarship. The data are tabulated in the main paper and in the supplementary materials.

**Author Contributions:** S.H. and P.D.H. oversaw all the work performed and wrote the manuscript, S.H., T.B.G. L.M.C and B.K.L performed the experiments, S.H., T.B.G., A.K., J.M.M., L.M.C and P.D.H. analyzed and interpreted the data.

**Author Information:** Reprints and permissions information is available at www.nature.com/reprints. The authors declare no competing financial interests.

Correspondence and requests for materials should be addressed to hodgkin@wehi.edu.au

## References


1. Marchingo, J.M. *et al.* T cell signaling. Antigen affinity, costimulation, and cytokine inputs sum linearly to amplify T cell expansion. *Science* **346**, 1123-1127 (2014).

2. Mescher, M.F. *et al.* Signals required for programming effector and memory development by CD8+ T cells. *Immunol Rev* **211**, 81-92 (2006).

3. Zehn, D., Lee, S.Y. & Bevan, M.J. Complete but curtailed T-cell response to very low-affinity antigen. *Nature* **458**, 211-214 (2009).

4. Hawkins, E.D., Markham, J.F., McGuinness, L.P. & Hodgkin, P.D. A single-cell pedigree analysis of alternative stochastic lymphocyte fates. *Proc Natl Acad Sci U S A* **106**, 13457-13462 (2009).

5. Turner, M.L., Hawkins, E.D. & Hodgkin, P.D. Quantitative Regulation of B Cell Division Destiny by Signal Strength. *The Journal of Immunology* **181**, 374-382 (2008).

6. Vervoorts, J., Lüscher-Firzlaff, J. & Lüscher, B. The Ins and Outs of MYC Regulation by Posttranslational Mechanisms. *Journal of Biological Chemistry* **281**, 34725-34729 (2006).

7. Laurenti, E. *et al.* Hematopoietic stem cell function and survival depend on c-Myc and N-Myc activity. *Cell stem cell* **3**, 611-624 (2008).

8. Donnelly, R.P. & Finlay, D.K. Glucose, glycolysis and lymphocyte responses. *Molecular Immunology* **68**, 513-519 (2015).

9. Preston, G.C. *et al.* Single cell tuning of Myc expression by antigen receptor signal strength and interleukin-2 in T lymphocytes. *Embo j* **34**, 2008-2024 (2015).

10. Wang, R. *et al.* The Transcription Factor Myc Controls Metabolic Reprogramming upon T Lymphocyte Activation. *Immunity* **35**, 871-882 (2011).

11. Liu, J. & Levens, D. Making myc. *Current topics in microbiology and immunology* **302**, 1-32 (2006).

12. Conacci-Sorrell, M., McFerrin, L. & Eisenman, R.N. An overview of MYC and its interactome. *Cold Spring Harb Perspect Med* **4**, a014357 (2014).

13. Dang, Chi V. MYC on the Path to Cancer. *Cell* **149**, 22-35 (2012).

14. Vita, M. & Henriksson, M. The Myc oncoprotein as a therapeutic target for human cancer. *Seminars in Cancer Biology* **16**, 318-330 (2006).

15. Adams, J.M. *et al.* The c-myc oncogene driven by immunoglobulin enhancers induces lymphoid malignancy in transgenic mice. *Nature* **318**, 533-538 (1985).

16. Ogilvy, S. *et al.* Constitutive Bcl-2 expression throughout the hematopoietic compartment affects multiple lineages and enhances progenitor cell survival.

*Proceedings of the National Academy of Sciences of the United States of America* **96**, 14943-14948 (1999).

17. Hawkins, E.D., Turner, M.L., Dowling, M.R., van Gend, C. & Hodgkin, P.D. A model of immune regulation as a consequence of randomized lymphocyte division and death times. *Proc Natl Acad Sci U S A* **104**, 5032-5037 (2007).

18. Gregory, M.A. & Hann, S.R. c-Myc Proteolysis by the Ubiquitin-Proteasome Pathway: Stabilization of c-Myc in Burkitt's Lymphoma Cells. *Molecular and Cellular Biology* **20**, 2423-2435 (2000).

19. Nie, Z. *et al.* c-Myc Is a Universal Amplifier of Expressed Genes in Lymphocytes and Embryonic Stem Cells. *Cell* **151**, 68-79 (2012).

20. Duffy, K.R. & Hodgkin, P.D. Intracellular competition for fates in the immune system. *Trends in Cell Biology* **22**, 457-464 (2012).

21. Duffy, K.R. *et al.* Activation-Induced B Cell Fates Are Selected by Intracellular Stochastic Competition. *Science* **335**, 338-341 (2012).

22. Hawkins, E.D. *et al.* Measuring lymphocyte proliferation, survival and differentiation using CFSE time-series data. *Nat Protoc* **2**, 2057-2067 (2007).

23. Kinjyo, I. *et al.* Real-time tracking of cell cycle progression during CD8+ effector and memory T-cell differentiation. *Nat Commun* **6**, 6301 (2015).

24. Marchingo, J.M. *et al.* T cell stimuli independently sum to regulate an inherited clonal division fate. *Nat Commun* **in press** (2016).

25. Raff, M. The mystery of intracellular developmental programmes and timers. *Biochemical Society Transactions* **34**, 663-670 (2006).

26. Burton, P.B.J., Raff, M.C., Kerr, P., Yacoub, M.H. & Barton, P.J.R. An Intrinsic Timer That Controls Cell-Cycle Withdrawal in Cultured Cardiac Myocytes. *Developmental Biology* **216**, 659-670 (1999).

27. Link, J.M. & Hurlin, P.J. The activities of MYC, MNT and the MAX-interactome in lymphocyte proliferation and oncogenesis. *Biochimica et Biophysica Acta (BBA) - Gene Regulatory Mechanisms* **1849**, 554-562 (2015).

28. Prendergast, G.C. Mechanisms of apoptosis by c-Myc. *Oncogene* **18**, 2967-2987 (1999).

29. Cory, S., Huang, D.C.S. & Adams, J.M. The Bcl-2 family: roles in cell survival and oncogenesis. *Oncogene* **22**, 8590-8607 (2003).

30. Strasser, A., Harris, A.W., Bath, M.L. & Cory, S. Novel primitive lymphoid tumours induced in transgenic mice by cooperation between myc and bcl-2. *Nature* **348**, 331-333 (1990).

31. Aukema, S.M. *et al.* Double-hit B-cell lymphomas. *Blood* **117**, 2319-2331 (2011).

32. Hommel, M. & Hodgkin, P.D. TCR affinity promotes CD8+ T cell expansion by regulating survival. *J Immunol* **179**, 2250-2260 (2007).

## Figure Legends

**Fig. 1**. **Regulation of Myc is a division independent, timed process. a,b,** Models of putative division promoting factor either diluted with each division **(a),** or progressively lost over time and unaffected by division **(b)**. **c-o,** Proliferation, division cessation and Myc expression of naive CTV-labelled C57BL/6 B cells stimulated with CpG **(c-f, j-l)** or OT-I/*Bcl2l11*$^{-/-}$ CD8$^{+}$ T cells stimulated with N4 peptide and 6.32µg/mL CD28 antibody **(g-i, m-o)**. CTV histograms **(c)**, total cell numbers **(d,g),** MDN over time **(e,h**) and geometric mean fluorescent intensity (gMFI) of intracellular Myc staining **(f,i)**. Dashed lines in (f,i) indicate DD times as estimated in (e,h) calculated as described in Supplementary Figure 1. **j-o,** Dot plots of CTV versus intracellular Myc staining at times indicated **(j,m)** and gMFI of intracellular Myc staining measured per division over time **(k,l,n,o).** (c,j,m) Representative dot plots of triplicate culture wells. (d-i,k,l,n-o) mean +/- SEM from triplicate culture wells. Data are from one experiment representative of 5 (B cells) or 3 (T cells) independent experiments with similar results.

**Fig. 2. Myc overexpression reveals independent regulation of death and destiny timers.** Division progression of CpG stimulated B cells from C57BL/6 **(a-c)** or Bcl-2-Tg **(d,e)** mice transduced with Myc-expressing or control GFP$^{+}$ retrovirus. Total cell number **(a,d)**, MDN over time **(b,e)** and dot plots of CTV versus GFP **(c).** (a,b,d,e) Data are shown for GFP positive cell populations, representing infected cells. Correlation of Myc protein expression with GFP levels is demonstrated in **Supplementary Fig. 2c,d**. (a,b,d,e) mean +/- SEM from triplicate culture wells. (c) Representative dot plots of triplicate culture wells. Data are from one experiment. Similar results were obtained by three independent experiments using WT B cells and one repeat experiment extending lifespan using Bim deficient B cells.

**Fig. 3. Strength and combination of stimuli determine Myc levels and DD. a,** Total cell number, **b**, MDN and **c,** gMFI of intracellular Myc staining over time in OT-I/*Bcl2l11*$^{-/-}$ CD8$^{+}$ T cells stimulated with N4 peptide and CD28 antibody at concentrations indicated. The time when division ceased for the weakest stimulation (N4) was estimated in (b) and is indicated as dashed line in (c). **d-g,** OT-I/*Bcl2l11*$^{-/-}$ CD8$^{+}$ T cells stimulated with N4 and 10U/mL IL-2 or 6.32µg/mL CD28 antibodies **(d-f)** or as indicated **(g)** for 23 h before being washed and further cultured without stimulation. **d,** Myc protein measured by flow cytometry at 23 h post stimulation. The line indicates mean Myc level measured in the weakest stimulation (N4). **e,** CTV proliferation profiles and **f,** MDN over time. Dashed lines in (e) indicate cells in generation 2 at 91 h. **g,** Correlation of DD with Myc protein levels measured at 23 hours after activation. **h,** Correlation of DD with Myc protein levels in B cells from *Bcl2l11*$^{-/-}$ mice stimulated for 23 hours with 500U/mL IL-4 and anti-CD40 antibodies as indicated before being washed and returned to culture with no further stimulation. (a-c,f-h) means +/- SEM from triplicate culture wells; (d,e) representatives of triplicate culture wells. Data are from one experiment representative of four (a-c), two (d-g) or one (h) independent experiments with similar results.

**Fig. 4. Time dependent regulation of Myc. a,** Myc protein and **b,** MDN over time of OT-I/*Bcl2l11*$^{-/-}$ CD8$^{+}$ T cells stimulated with N4 and CD28 antibody as indicated. Times to DD indicated by dashed lines were estimated in (b) as described in Supplementary Figure 1. **c,** Decay curves fitted to Myc levels during the loss phase. gMFI data from (b) were log transformed and straight lines with the same decay rate fitted to data points displayed in the graph. Red circles indicate intersection of estimated DD time with fitted lines for each condition. Red dashed line indicates a putative common Myc DD threshold. **d,** OT-I/*Bcl2l11*$^{-/-}$ CD8$^{+}$ T cells stimulated with N4 and 20 µg/mL anti-CD28 antibody or 100 U/mL h-IL-2 as

indicated were treated with CHX at indicated time points and Myc levels measured for 6 hours. Calculated half-lives are displayed below each time point and 95% confidence intervals given in Supplementary Table 1. (a-d) mean +/- SEM from triplicate culture wells. Data are from one experiment representative of three (a-c) or two (d) independent experiments with similar results.

**Fig. 5. Myc levels before first division determine DD. a-c,** $CD8^+$ T cells stimulated with N4 and 6.32µg/mL anti-CD28 antibodies or **d-e,** B cells stimulated with CpG from OT-I-Myc-EGFP mice were cultured for 24 hours before being sorted on high forward scatter and 3 levels of EGFP as reporter for Myc levels. Sorted cells were further cultured without stimulation. **a,d,** EGFP levels after sorting, **b,e,** cell numbers and **c,f,** MDN over time. (b,c,e,f) mean +/- SEM from triplicate culture wells. Data are from one experiment representative of two independent experiments for B cells and a repeat for T cells stimulated with anti-CD3 and 6.32µg/mL anti-CD28.

**Fig. 6. Inhibition of division times has no effect on DD and death timers. a-d,** MPA was added to CTV labelled OT-I/*Bcl2l11*$^{-/-}$ $CD8^+$ T cells stimulated with N4 and IL-2. MPA effect on cell numbers (**a**), MDN (**b**) (Supplementary Figure 1 and [22, 32]) and precursor cohort number (**c**) over time. When adjusted for cell expansion, cells are dying at similar rates conforming to a right-skewed distribution (**c,d**). Data for cells without drug (left panel) were fitted to 1-cumulative lognormal (m = 4.17; s = 0.36) (shown in panel (d)). This survival curve is overlaid to the data with 100 or 200 ng/ml MPA (center and right panel in (c)). (a,b) mean +/- SEM from triplicate culture wells. Data are from one experiment representative of two independent experiments with similar results.

**Fig. 7. Model for timed fates controlling the early immune response. a,** Signal combinations determine the rate of production of Myc over time (green intensity). **b,** The molecular machinery regulating DD is modelled as a temporal controller insensitive to division. **c,** Single cell fate is determined by competing timers for division and death. For this cell and all progeny, DD and division cessation is reached at 40h and death at 60h. **d,** Example of population based distributions in times to first division (blue line), DD driven by Myc (green line) and death (red line) timers. **e,** Unconstrained division would lead to unlimited increase in cell numbers (blue line). Constraining cell division by DD alone leads to a plateau (green line). The combination of division, DD and death timers forms the typical shape of an immune response (red line). **f,** Data from retroviral infections (**Fig. 2)** are fitted by model (circles are data, lines are from model with parameters depicted in distributions on right). Control retrovirus (vector) infected wild-type or Bcl-2-Tg cells have identical parameters for DD time (green lines in right panels) (distribution *a*) while wild-type cells infected with control or Myc-expressing retrovirus have the same parameters for survival (red lines in right panels) (distribution *b*). Summing both changes (Myc, distribution *c* and Bcl-2 distribution *d*) predicts net cell number for Myc in Bcl-2-Tg cells (purple dots and line; parameters in Supplementary Discussion). **g,** Effects of 20% changes to either DD or survival times alone or together on cell number over time.

## Materials and Methods

### Mice:

Mice deficient for Bim (*Bcl2l11*$^{-/-}$)[33], Bcl-2-Tg (VavP-BCL2-69) and Eμ-Myc mice were a gift from Philippe Bouillet (WEHI). Myc-EGFP (*Myc*$^{tm1.1Dlev}$/J) were purchased from Jackson Laboratories. *Bcl2l11*$^{-/-}$ and Myc-EGFP mice were bred with ovalbumin transgenic class I (OT-I) mice from the WEHI animal facility (Kew, Victoria, Australia) to create OT-I/*Bcl2l11*$^{-/-}$ and OT-I/Myc-EGFP respectively. VavP-Myc10 homozygous mice[34] were a gift from Suzanne Cory (WEHI). C57BL/6 and C57BL/6-Ly5.1 were originally obtained from Jackson Laboratories and maintained at the WEHI animal facility for > 5 generations. All mice were bred and maintained under specific pathogen-free conditions in the WEHI animal facilities (Parkville, Victoria, Australia) and used between 6-12 weeks of age. All experiments were performed under the approval of the WEHI Animal Ethics Committee.

### B and T cell culture:

B or T cells were cultured in lymphocyte culture medium made of RPMI-1640, supplemented with 10% (vol/vol) FBS, 10 mM Hepes, 100 U/mL penicillin, 100 μg/mL streptomycin, 2mM GlutaMAX, 0.1mM non-essential amino acids, 1mM sodium pyruvate (all Invitrogen), and 50 μM β-2-mercaptoethanol (Sigma).

For B cell stimulations, small resting B cells were isolated using an established protocol[17] with a discontinuous Percoll (GE Healthcare) gradient and negative magnetic bead isolation kit (EasySep Mouse B-cell isolation kit, Stemcell Technologies or B cell isolation kit, Miltenyi Biotech). Purity was typically >95% (B220$^+$ CD19$^+$ and IgM$^+$ or IgD$^+$). B cells were stimulated either with 3 μM CpG 1668 (sequence 5'TCCATGACGTTCCTGATGCT-3', Geneworks) or with 500 U/mL IL-4 (baculovirus-transfected Sf21 insect cell supernatant, WEHI) and anti-CD40 antibody (clone 1C10, WEHI monoclonal antibody facility) at concentrations indicated.

$CD8^+$ T cells were isolated from mouse lymph nodes (inguinal, axillary, brachial, and superficial cervical) by negative selection using the EasySep Mouse $CD8^+$ T cell Isolation kit (StemCell Technologies). Purity was typically > 95% ($CD8^+$ for cells from non-TCR-Tg mice and $CD8^+V\alpha2^+$ for cells from OT-I TCR-Tg mice). $CD8^+$ T cells were stimulated with plate-bound anti-CD3 antibody (10µg/mL, clone 145-2C11, WEHI monoclonal antibody facility). OT-I TCR-Tg $CD8^+$ T cells were stimulated with 0.01µg/mL SIINFEKL peptide (N4) (Auspep). Anti-CD28 antibody (clone 37.51, WEHI monoclonal antibody facility) or human IL-2 (h-IL-2) (Peprotech) were added to the cultures as indicated. All T cell cultures contained 25µg/mL anti-mouse IL-2 antibody (clone S4B6, WEHI monoclonal antibody facility) which blocks the activity of mouse IL-2 *in vitro* but does not recognize h-IL-2[35].

To track cell division, cells were labelled with 5µM CellTrace Violet (CTV) (Invitrogen) according to manufacturer instructions. Cells were seeded at $1x10^4$cells/well and cultured in 96 well plates.

**Flow cytometry, Cell counting:**

Flow Cytometry was performed on FACSCanto II or Fortessa X-20 cytometer (both BD Biosciences). Data was analyzed using FlowJo software (Treestar). A known number of beads (Rainbow calibration particles BD Biosciences) were added to samples immediately prior to analysis and the ratio of beads to live cells was used to calculate the absolute cell number in each sample. Propidium iodide (0.2µg/mL, Sigma) were used for dead cell exclusion.

In co-culturing experiments of T cells from vavP-Myc10 and from C57BL/6-Ly5.1 mice, Ly.5-1-PE (clone A20, BD Biosciences) and Ly5.2-FITC (clone 104, eBioscience) antibodies were added to the bead suspension to distinguish between these two cell types.

**Flow cytometric cell sorting:**

Cell sorting of T and B cells from OT-I-Myc-EGFP was done on a BD FACSARIA III (BD Biosciences). Cells were harvested 24 h after activation. Cells falling into the top 25% of the Forward Scatter range (measuring cell size indicative for activation level) were sorted into 3 levels of EGFP expression as marker for Myc levels. After cell sorting cells were re-cultured in lymphocyte culture medium without further stimulation.

**Intracellular staining for Myc:**

For intracellular staining of Myc protein cells were harvested at time points indicated and immediately stored in fixation buffer at 4°C for at least 16h until staining was performed. Staining of all fixed samples within one experiment was performed at the same time. Fixation buffer contained 0.5% paraformaldehyde, 0.2% Tween-20 and 0.1% bovine serum albumin in PBS. For staining, samples were split into two wells to be incubated for 60 min with either anti-Myc antibody (clone D84C12, Cell Signaling) or a rabbit IgG isotype control (clone D1AE, Cell Signaling). Cell were washed and incubated for 60 min with an anti-rabbit IgG conjugated to Alexa Fluor 647 (A-647). Cells were washed and analyzed by flow cytometry.

**Retroviral vector production:**

A fragment encoding the mouse c-myc open reading frame (MGI:97250) was synthesized (DNA 2.0, Ca, USA), flanked by BamHI and EcoRI sites, and cloned into the retroviral vector pMX-pie[36]. Native Myc is expressed from this cassette along with GFP, downstream of an IRES. The vector also confers puromycin resistance.

To generate retroviral supernatants, 293T cells were transfected with the constructs described above, viral gag and pol using X-tremeGENE 9 DNA transfection reagent (Roche). Viral supernatants were harvested and frozen for further use.

**Retroviral infection:**

For retroviral infection B cells were harvest 24 h after activation. Viral supernatant was thawed and 50µM 2-Mercaptoethanol and 100mM polyprene added. Cells were resuspended in viral supernatant and spin-infection was performed at 2400g, at 37°C for 2h. After infection cells were re-cultured in lymphocyte culture medium without further stimulation. This method is not suitable for T cells as they have very low rates of infection.

**Estimation of MDN:**

The MDN is calculated using the precursor cohort method as described in [1]. Briefly the precursor cohort method removes the effect of cell division on the total cell numbers by dividing the cell number in division *i* by $2^i$ to obtain a cohort number for that division ($C_i$).

The 'total cohort number' at any given time point is the sum of all cohort numbers at this time point:

$$\text{total cohort number} = C_0+C_1+C_2+C_3+... +Cn$$

with n = the highest division measured.

The 'mean division number' is then calculated as:

$$MDN = (C_1+C_2*2+C_3*3+.....+C_n*n)/\text{total cohort number}$$

with n= maximum number of divisions cells measured.

Note that maximum number of 7-8 divisions can be traced using cell division tracking dyes such as CTV.

**Estimation of DD and DD times:**

The maximum mean division number (DD) and the time for a cell population to stop dividing (DD time) is estimated using mean division number (MDN) versus time plots as described in Supplementary Figure 1.

**Methods-only references**


33. Bouillet, P. *et al.* Proapoptotic Bcl-2 Relative Bim Required for Certain Apoptotic Responses, Leukocyte Homeostasis, and to Preclude Autoimmunity. *Science* **286**, 1735-1738 (1999).

34. Smith, D.P., Bath, M.L., Metcalf, D., Harris, A.W. & Cory, S. MYC levels govern hematopoietic tumor type and latency in transgenic mice. *Blood* **108**, 653-661 (2006).

35. Deenick, E.K., Gett, A.V. & Hodgkin, P.D. Stochastic model of T cell proliferation: a calculus revealing IL-2 regulation of precursor frequencies, cell cycle time, and survival. *J Immunol* **170**, 4963-4972 (2003).

36. Liu, X. *et al.* Generation of mammalian cells stably expressing multiple genes at predetermined levels. *Analytical biochemistry* **280**, 20-28 (2000).

# Fig. 1

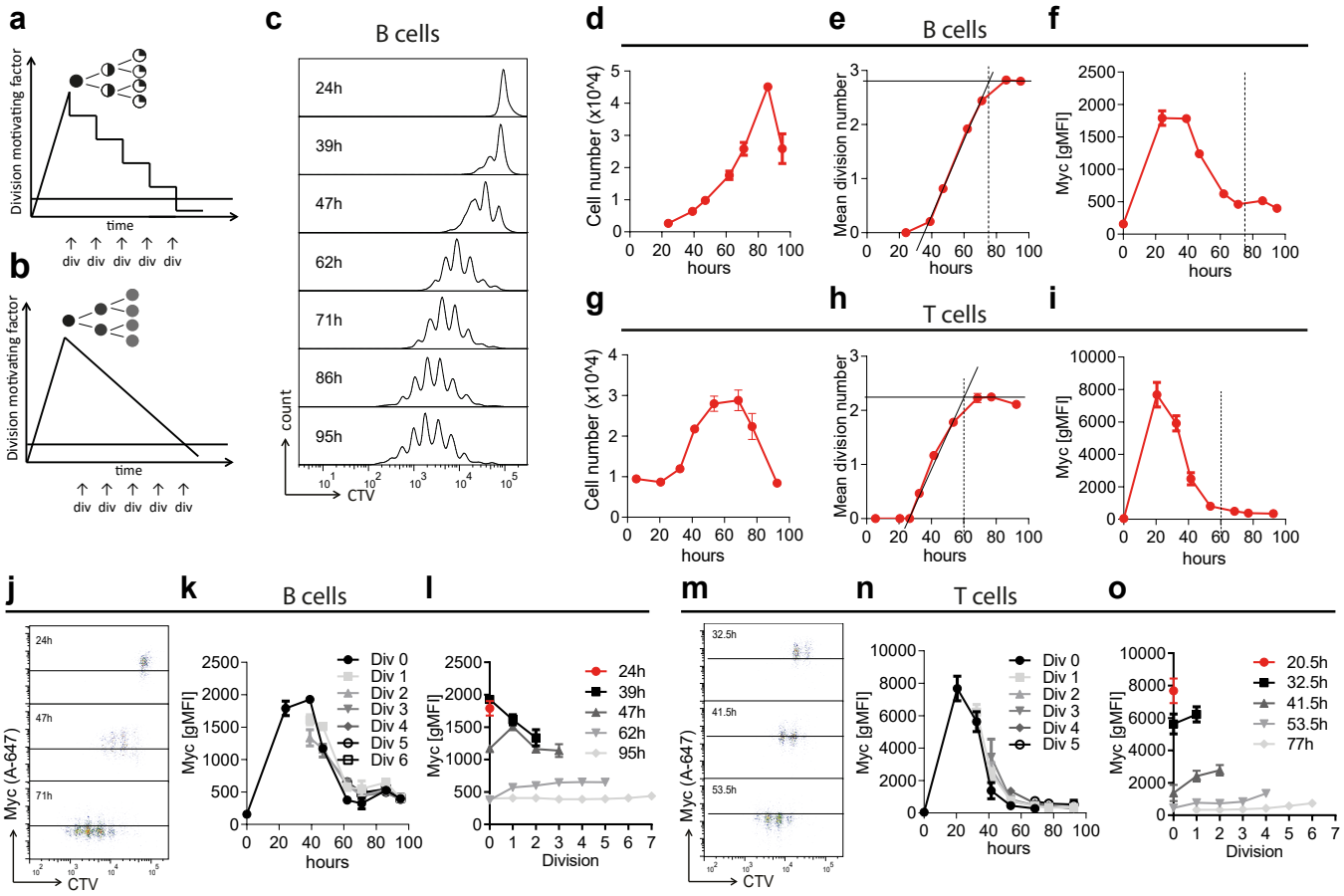
a
Division motivating factor
time
div div div div div
b
Division motivating factor
time
div div div div div
c
B cells
24h
39h
47h
62h
71h
86h
95h
count
CTV
d
Cell number (x10^4)
hours
e
B cells
Mean division number
hours
f
Myc [gMFI]
hours
g
Cell number (x10^4)
hours
h
T cells
Mean division number
hours
i
Myc [gMFI]
hours
j
24h
47h
71h
Myc (A-647)
CTV
k
B cells
Myc [gMFI]
Div 0
Div 1
Div 2
Div 3
Div 4
Div 5
Div 6
hours
l
Myc [gMFI]
24h
39h
47h
62h
95h
Division
m
32.5h
41.5h
53.5h
Myc (A-647)
CTV
n
T cells
Myc [gMFI]
Div 0
Div 1
Div 2
Div 3
Div 4
Div 5
hours
o
Myc [gMFI]
20.5h
32.5h
41.5h
53.5h
77h
Division

# Fig. 2

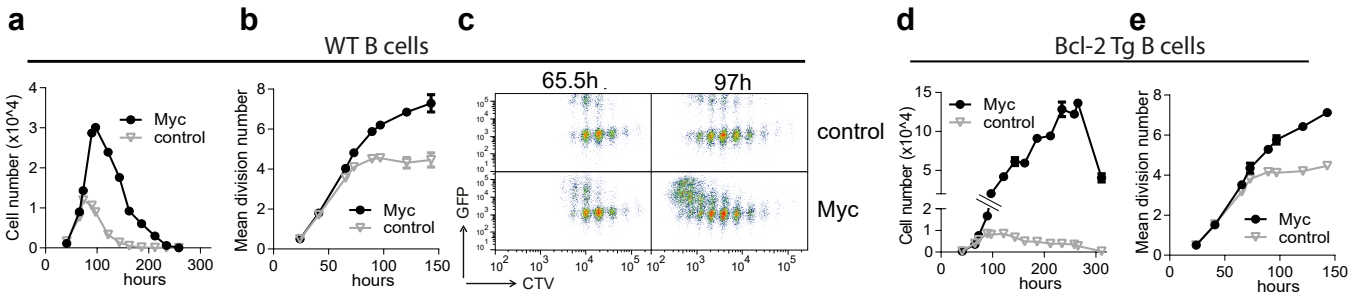
a
b
c
d
e
WT B cells
Bcl-2 Tg B cells
Cell number (x10^4)
Mean division number
hours
Myc
control
65.5h
97h
GFP
CTV
control
Myc

# Fig. 3

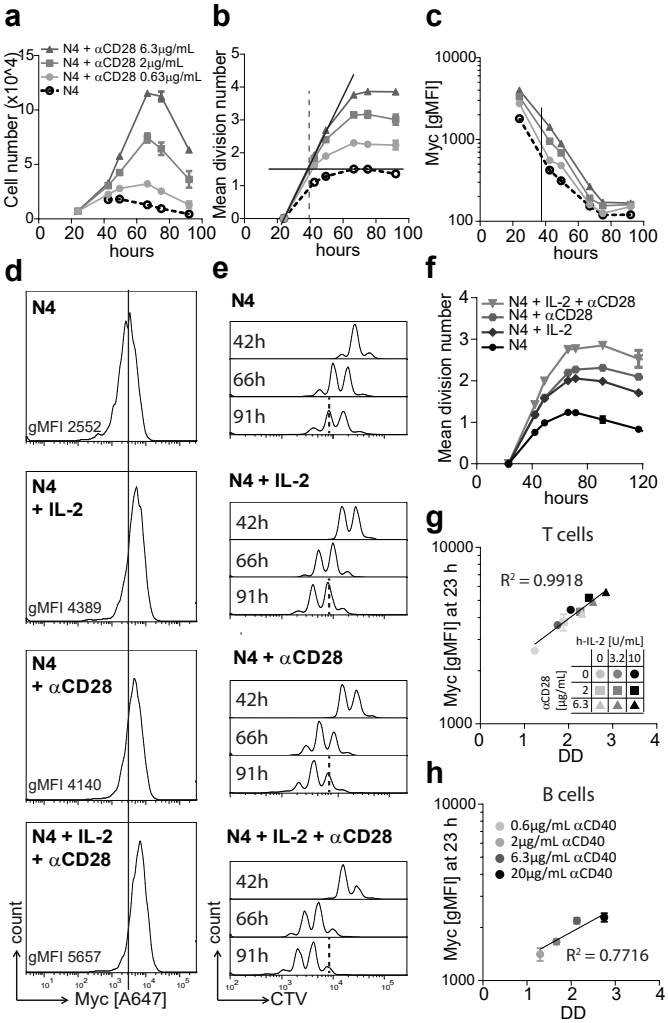
a
b
c
N4 + αCD28 6.3μg/mL
N4 + αCD28 2μg/mL
N4 + αCD28 0.63μg/mL
N4
Cell number (x10^4)
Mean division number
Myc [gMFI]
hours
d
e
f
N4
gMFI 2552
N4 + IL-2
gMFI 4389
N4 + αCD28
gMFI 4140
N4 + IL-2 + αCD28
gMFI 5657
42h
66h
91h
N4 + IL-2
N4 + αCD28
N4 + IL-2 + αCD28
count
Myc [A647]
CTV
Mean division number
hours
g
T cells
Myc [gMFI] at 23 h
R² = 0.9918
h-IL-2 [U/mL]
αCD28 [μg/mL]
DD
h
B cells
0.6μg/mL αCD40
2μg/mL αCD40
6.3μg/mL αCD40
20μg/mL αCD40
R² = 0.7716

# Fig. 4

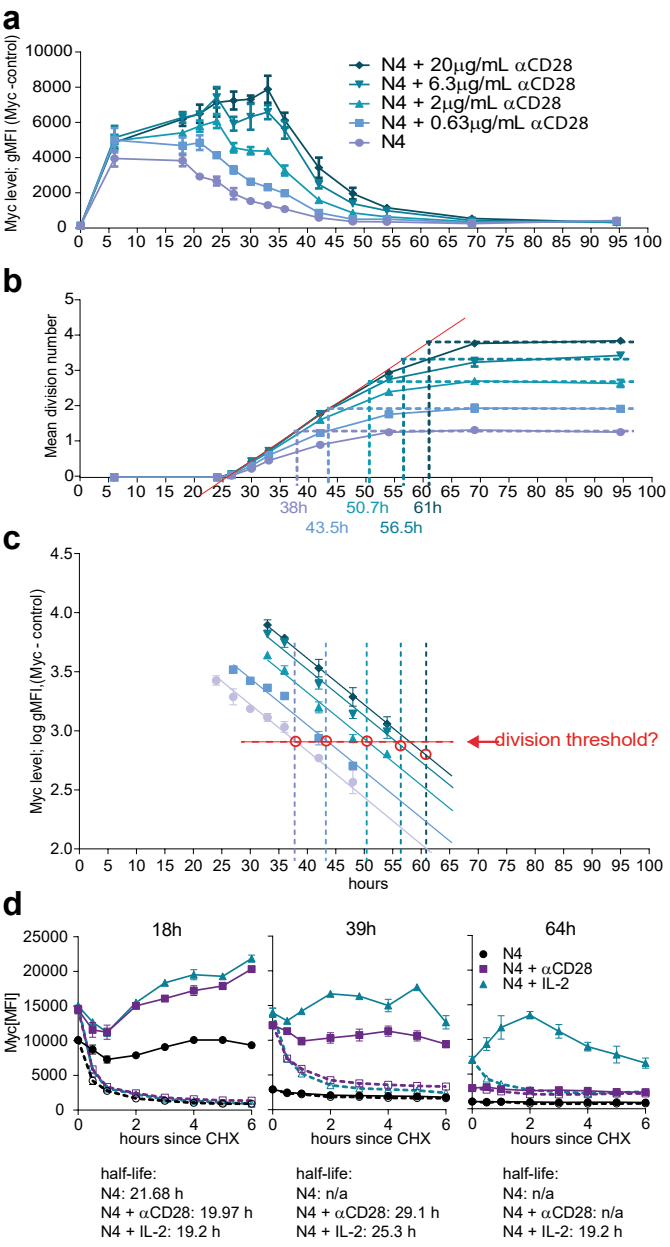
a
Myc level; gMFI (Myc -control)
N4 + 20μg/mL αCD28
N4 + 6.3μg/mL αCD28
N4 + 2μg/mL αCD28
N4 + 0.63μg/mL αCD28
N4
b
Mean division number
38h
43.5h
50.7h
56.5h
61h
c
Myc level; log gMFI (Myc - control)
division threshold?
hours
d
18h
39h
64h
N4
N4 + αCD28
N4 + IL-2
Myc[MFI]
hours since CHX
half-life:
N4: 21.68 h
N4 + αCD28: 19.97 h
N4 + IL-2: 19.2 h
half-life:
N4: n/a
N4 + αCD28: 29.1 h
N4 + IL-2: 25.3 h
half-life:
N4: n/a
N4 + αCD28: n/a
N4 + IL-2: 19.2 h

# Fig. 5

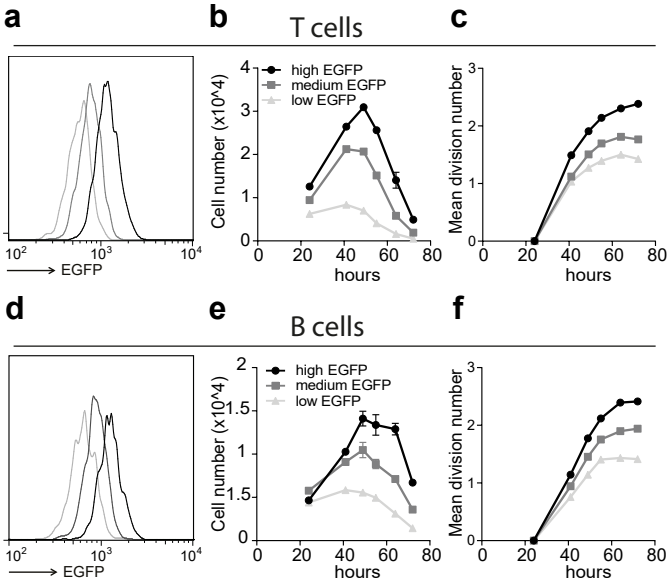
a
b
T cells
c
high EGFP
medium EGFP
low EGFP
Cell number (x10^4)
Mean division number
hours
EGFP
d
e
B cells
f

# Fig. 6

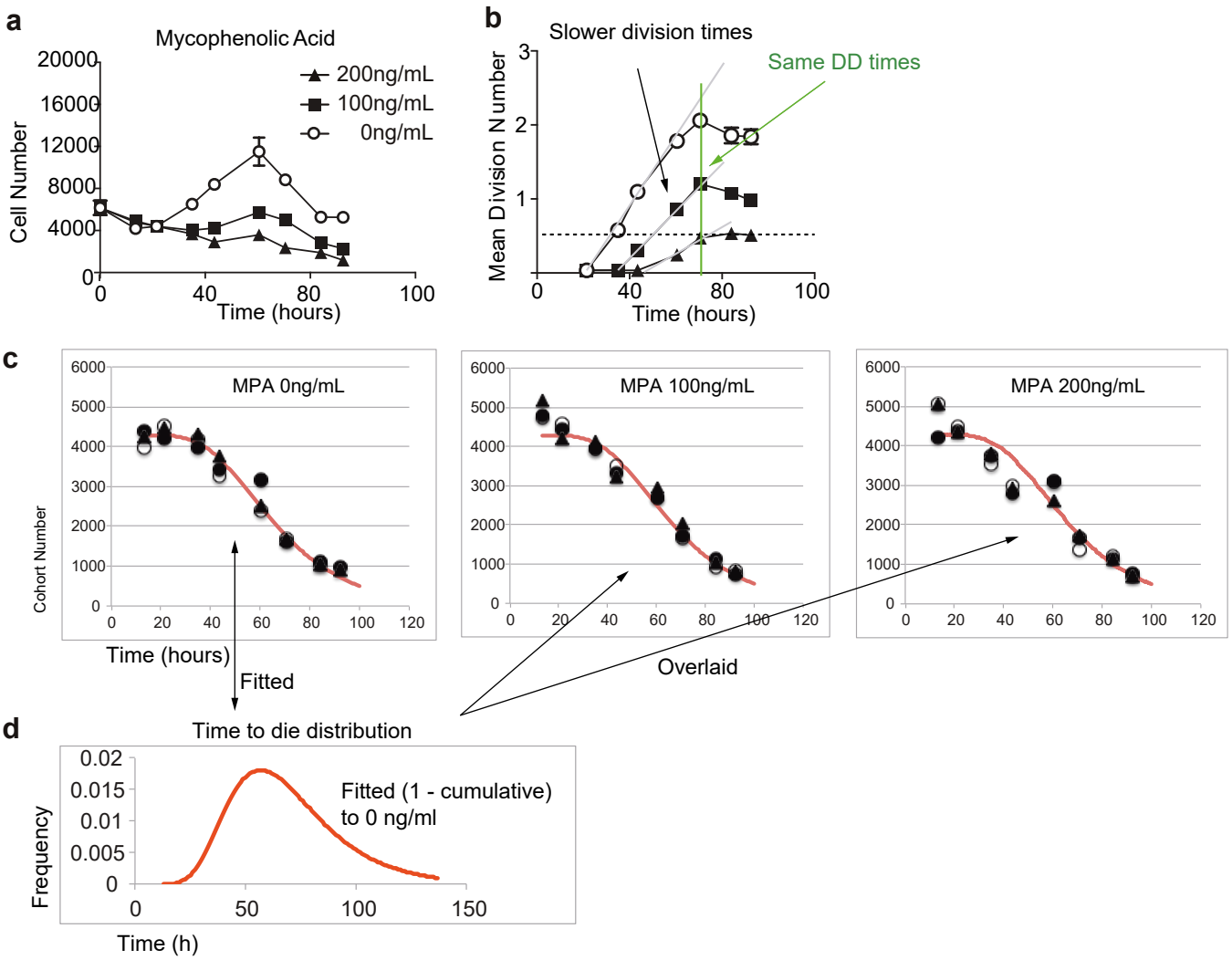
a
Mycophenolic Acid
200ng/mL
100ng/mL
0ng/mL
Cell Number
Time (hours)
b
Slower division times
Same DD times
Mean Division Number
Time (hours)
c
MPA 0ng/mL
MPA 100ng/mL
MPA 200ng/mL
Cohort Number
Time (hours)
Fitted
Overlaid
d
Time to die distribution
Fitted (1 - cumulative)
to 0 ng/ml
Frequency
Time (h)

# Fig. 7

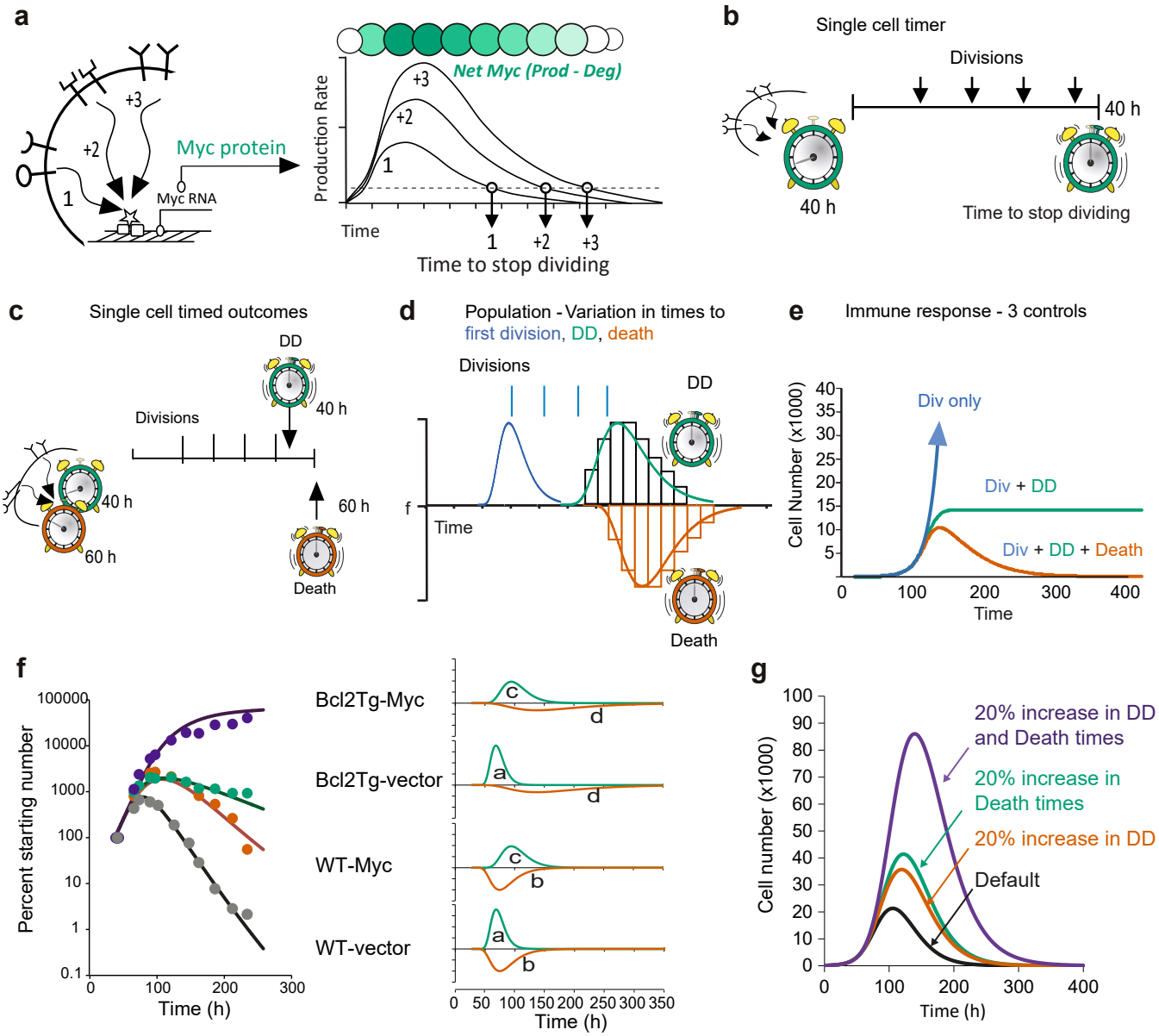
a
+3
+2
1
Myc protein
Myc RNA
Net Myc (Prod - Deg)
Production Rate
Time
Time to stop dividing
b
Single cell timer
Divisions
40 h
Time to stop dividing
c
Single cell timed outcomes
DD
Divisions
40 h
60 h
Death
d
Population - Variation in times to
first division, DD, death
Divisions
DD
f
Time
Death
e
Immune response - 3 controls
Div only
Div + DD
Div + DD + Death
Cell Number (x1000)
Time
f
Percent starting number
Time (h)
Bcl2Tg-Myc
Bcl2Tg-vector
WT-Myc
WT-vector
Time (h)
g
20% increase in DD
and Death times
20% increase in
Death times
20% increase in DD
Default
Cell number (x1000)
Time (h)

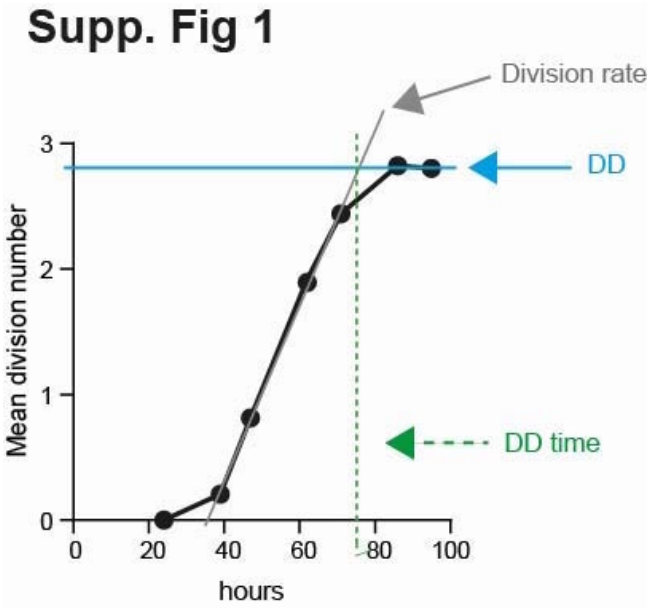


**Supplementary Figure 1**

**Estimation of DD and DD times.**

The time for a cell population to stop dividing is estimated using a mean division number (MDN) versus time plot. MDN at any given time point is calculated using the precursor cohort model as described in1. When the cell population reaches DD the MDN plateaus. The mean DD of the population is defined as the maximum MDN reached by the population. The maximum mean division number is estimated by the highest point in the MDN over time curve as indicated by the solid blue line. The division rate is estimated from the slope of a line fitted (grey solid line) through at least 3 consecutive data points with increasing MDN values. Time to destiny (DD time) is estimated to be at the intersection of maximum MDN with the division rate as indicated by the green dashed line.

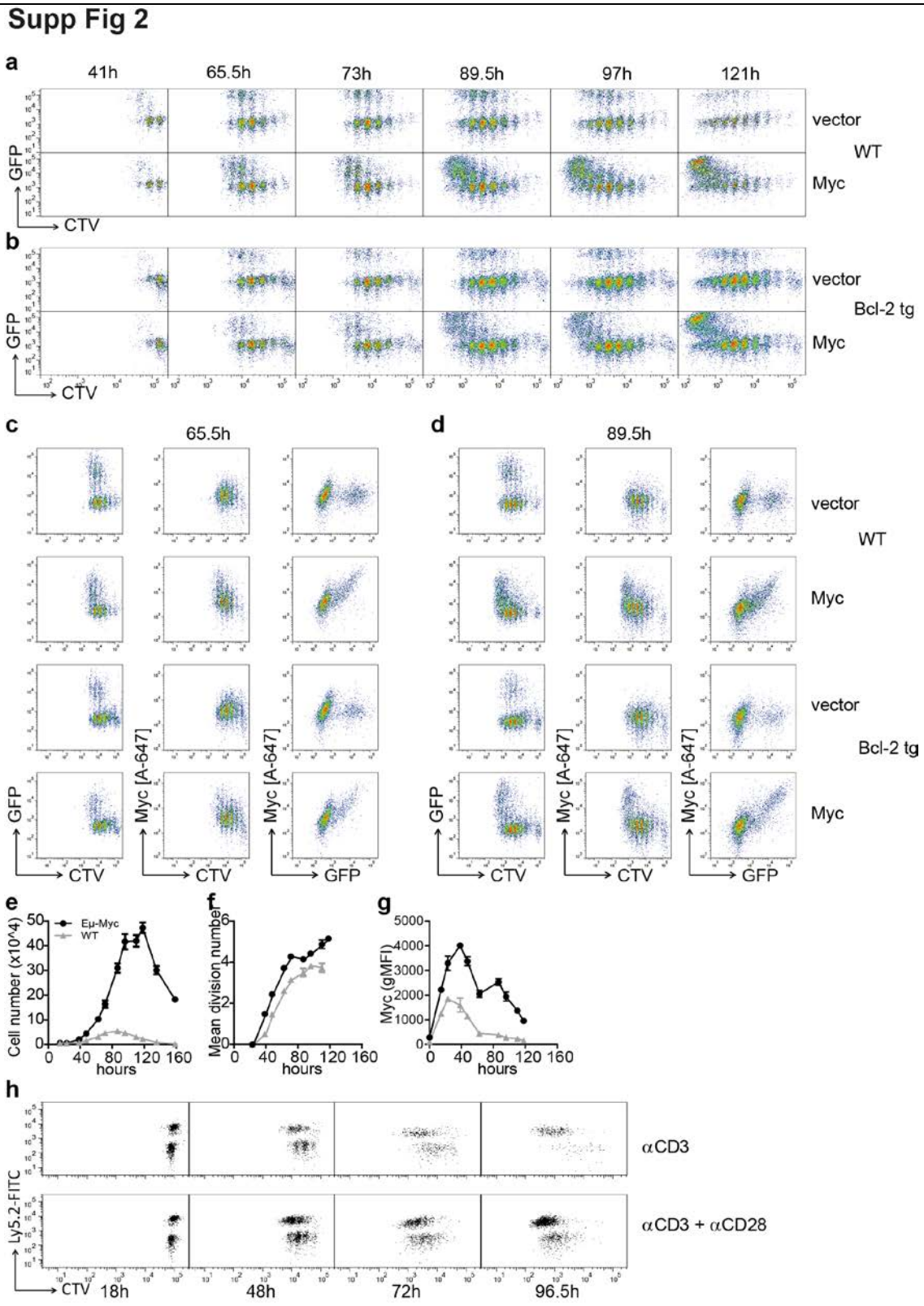


**Supplementary Figure 2**

**Forced expression of Myc drives division progression in B and T cells.**

Time course of CTV labelled B cells from **(a)** C57BL/6 or **(b)** Bcl-2-Tg mice stimulated with CpG for 24 h before infection with control (top panel) or Myc-expressing (bottom panel) $GFP^+$ retroviruses as in (Fig. 2). **c, d**, Myc protein expression was measured by intracellular staining in B cells transduced with $GFP^+$ retrovirus as in (a, b). Representative plots measured at **(c)** 65.5h or **(d)** 89.5h post activation with CpG. Only cells transduced with retrovirus expressing Myc ($GFP^+$ population) show elevated and sustained Myc protein expression in both WT and Bcl-2-Tg cells. **e,** Total cell number, **f,** MDN and **g,** Myc protein levels measured by flow cytometry over time in CTV labelled CpG stimulated B cells from Eμ-Myc mice (black circles) or C57BL/6 (WT) mice (grey triangles). At 48h post activation cells were split into new culture wells and fresh media was provided. **h,** Representative dot plots of CTV labelled $CD8^+$ T cells from vavP-Myc10 mice expressing congenic marker Ly5.2 co-cultured with CTV labelled $CD8^+$ T cells from C57BL/6-Ly5.1 (expressing Ly5.1 congenic marker, WT) mice. Cells were stimulated with plate bound anti-CD3 alone (top panel) or in combination with anti-CD28 (bottom panel). Cells were stained with an anti-Ly5.2-FITC (shown) and Ly5.1-PE antibody to distinguish vavP-Myc10 T cells from WT T cells. (a-d, h) Representative of triplicate culture wells, except for anti-CD3 stimulation alone at 72 hours and 96.5hours in (h), where flow cytometry profiles from triplicates were overlaid due to low event numbers. (e-g) mean +/- SEM from triplicate culture wells.

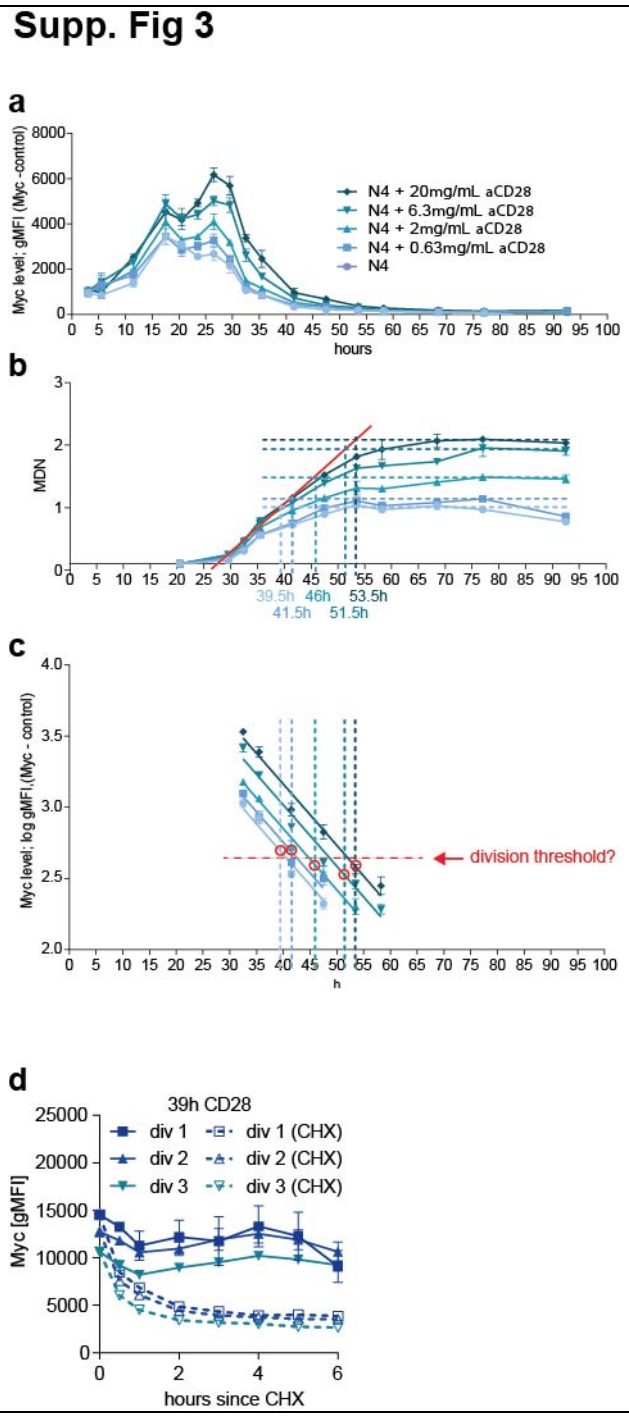


**Supplementary Figure 3**

**Time dependent regulation of Myc**

**a-c,** Repeat experiment of Fig 4**. a,** Myc protein and **b,** MDN over time of OT-I/ *Bcl2l11*$^{-/-}$ CD8$^{+}$ T cells stimulated with N4 and CD28 antibody as indicated. Times to DD indicated by dashed lines were estimated in (b) as described in Supplementary Figure 1. **c,** Decay curves fitted to Myc levels during the loss phase. gMFI data from (b) were log transformed and straight lines with the same decay rate forced fitted to data points displayed in the graph. Red circles indicate intersection of estimated DD time with fitted lines for each condition. Red dashed line indicates a putative common Myc DD threshold. **d,** Addition of CHX (dotted lines) to OTI/ *Bcl2l11*$^{-/-}$ CD8$^{+}$ T cells stimulated with N4 and 20 µg/mL CD28 antibody and followed for 6 hours revealed that half-life of Myc is independent of division (data shown in (d) are from experiment shown in Fig 4). (a-d) mean +/- SEM from triplicate culture wells.

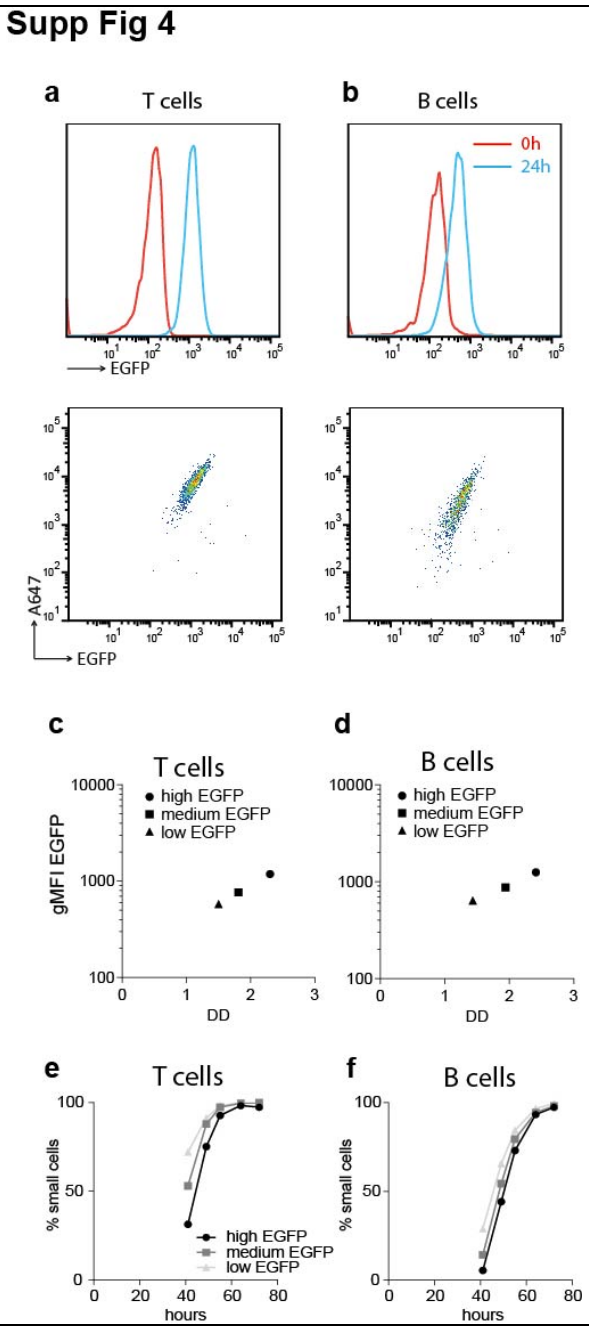


**Supplementary Figure 4**

**Use of T and B cells from OT-I-Myc-EGFP reporter reveals that DD is controlled by Myc-levels prior to first division.**

**a, b** Induction of EGFP after 24h of stimulation compared to unstimulated cells (top panels) and correlation of EGFP with Myc protein levels as determined by intracellular staining and flow cytometry (bottom panels) at 24h post stimulation in **(a)** $CD8^+$ T cells stimulated with N4 and 2µg/mL CD28 antibodies or **(b)** CpG stimulated B cells from OT-I-Myc-EGFP mice. **(c-f)** Level of Myc before first division determines DD. Data shown are from experiment shown in Fig. 5. Cells were stimulated for 24 hours with N4 and 6.32µg/mL CD28 antibodies (T cells, as in Fig. 5a-c) or CpG (B cells, as in Fig. 5 d-f) before being sorted on high FSC and high, medium or low levels of EGFP as reporter for Myc and placed back into culture without further stimulation. **c, d,** Correlation of DD with EGFP levels expressed after sorting of T cells (c) or B cells (d) from OT-I-Myc-EGFP mice. Correlation $r^2$, 0.99 and 0.95 for T and B cells respectively. **e, f,** Percent of small cells as measured by FSC as described in[1] as a surrogate marker for cells that have returned to quiescence in **(e)** T cells or **(f)** B cells. (a, b) Representative of triplicate culture wells (c, d) DD calculated as mean +/- SEM from triplicate culture wells plotted versus EGFP measured after sorting. (e, f) mean +/- SEM from triplicate culture wells.

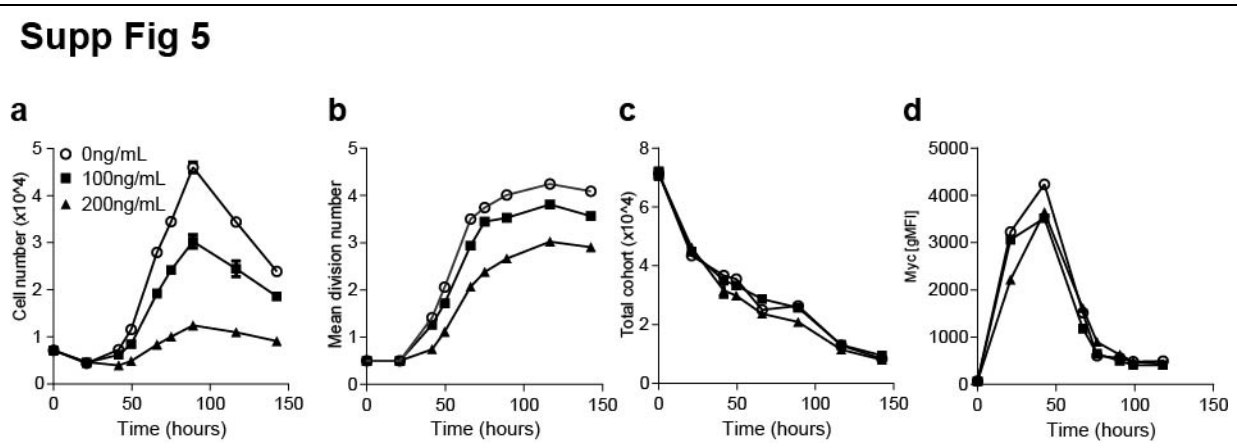


**Supplementary Figure 5**

**Alteration of division times by MPA has no effect on Myc levels, destiny and death timers.**

**a, b** MPA inhibits cell expansion over time (a) by slowing division times (b) in CTV labelled OTI/ *Bcl2l11*$^{-/-}$ CD8$^{+}$ T cells stimulated with N4 and IL-2. **c, d** MPA does not affect cell survival as measured by total cohort number over time (calculated by dividing the number of cells per division by 2^division number and representing the number of cells contributing to the cell population as indicator for cell death over time) (c) or Myc protein levels (d). (a-d) mean +/- SEM from triplicate culture wells.

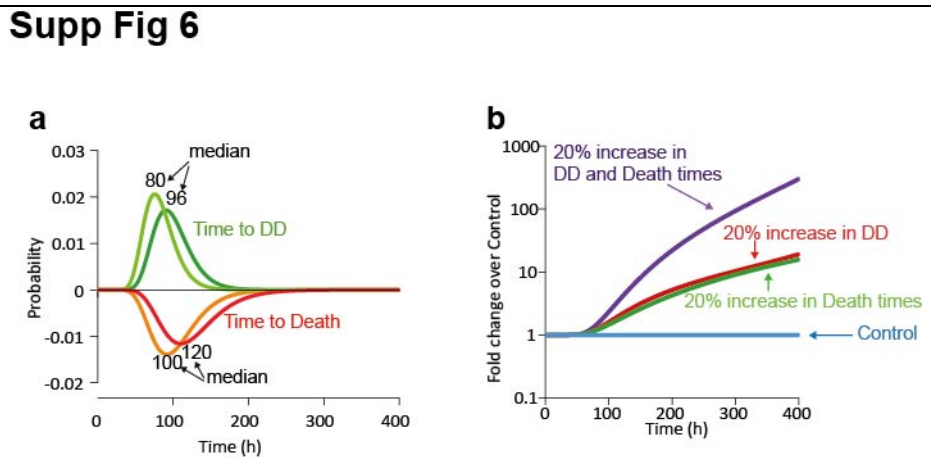


**Supplementary Figure 6**

**Sensitive regulation of cell numbers by changes to DD and time to die.**

**a,** Shows the lognormal distributions used to generate Fig. 4c where medians for times to reach DD and times to die are altered by 20% as shown. The calculated outcome for cell numbers with either change alone or together are plotted in Fig. 7g. Note, here the probability of dying is plotted as a negative pdf after Hawkins et al.[22]. Additional parameters of model are given in Supplementary Note 1. **b,** The fold differences in calculated cell numbers for each alteration over time are shown.

# Supplementary Information for Heinzel et al.:

# A Myc-dependent division timer complements a cell death timer to regulate T and B cell responses

**Supplementary Table 1.**

| **18h** | half-life (min) | 95% confidence |
|---|---|---|
| N4 | 21.68 | 19.48 to 24.43 |
| N4 + CD28 | 19.97 | 18.31 to 21.95 |
| N4 + IL-2 | 19.2 | 17.65 to 21.04 |

| **39h** | half-life (min) | 95% confidence |
|---|---|---|
| N4 | 44.54 | 29.05 to 95.42 |
| N4 + CD28 | 29.1 | 26.77 to 31.89 |
| N4 + IL-2 | 25.3 | 23.20 to 27.83 |

| **64h** | half-life (min) | 95% confidence |
|---|---|---|
| N4 | 52.36 | 25.32 to +infinity |
| N4 + CD28 | 38.99 | 28.35 to 62.44 |
| N4 + IL-2 | 28.51 | 24.32 to 34.45 |

**Half-life of Myc protein is relatively stable and independent of stimulation strength.** OT-I/*Bcl2l11*$^{-/-}$ CD8$^{+}$ T cells stimulated with N4 alone or in combination with 20 µg/mL anti-CD28 antibody or 100 U/mL h-IL-2 were treated with cycloheximide to block protein synthesis at indicated time points and Myc levels followed by flow cytometry for 6 hours. Half-life was estimated by fitting exponential decay curves.

**Supplementary Note 1**

Modelling T and B cell proliferation

The introduction of cellular timers for division and death that are unaffected by passage through mitosis (illustrated in Fig. 7) allows the development of a family of quantitative models. At the most basic level we can ignore individual cell variation and describe the cell response by the action of three cellular machines governing times to different fates: (i) division; (ii) division destiny; and (iii) death. Presumably activation takes some time to 'program' the DD and death times and to initiate the first division. Thus, we introduce the 'time for cell reprogramming' ($t_a$) *w*here the times for division, DD and death are set after activation. We have that cell number before $t_a$ is equal to the starting cell number ($n_0$), and cell number at any time *t* counted after $t_a$ can be given by the deterministic equations:

$$n(t) = \begin{cases} n_0 2^{\lfloor \min(t, t_{dd})/t_s \rfloor} & t < t_{dth} \\ 0 & t \geq t_{dth} \end{cases} \qquad (1)$$

Here $n(t)$ is the total live cell number, $t_{dth}$ is the global death time after which no cells survive, $t_{dd}$ is the division destiny time after which no cells divide, and $t_s$ is the time it takes each cell to divide (intermitotic time). Note that the square brackets here denote the floor function.

Furthermore, the quiescent cells ($q$) are the subset of live cells that have reached their DD:

$$q(t) = \begin{cases} n_0 2^{\lfloor t_{dd}/t_s \rfloor} & t_{dd} \geq t \geq t_{dth} \\ 0 & otherwise \end{cases} \qquad (2)$$

The deterministic equations above capture the principles of cellular operation, but are not suited to accurately describe a population of cells. Intercellular heterogeneity is a striking feature of lymphocytes that must be taken into account for accurate model development, even if the source of that variation is not known (ie. see [17, 37]). It is also necessary to determine whether there is any correlation in function (for example between times to divide, times to destiny and times to die) in individual cells and cell families and incorporate such correlations into a model for complete accuracy. These correlations are incompletely known and require further experiment, such as through tracking family outcomes with video microscopy, to be determined. If, as a first approximation, we assume the machinery for division, destiny and death are independent we could express the deterministic equation 1 as its equivalent stochastic equation (not shown).

In a stochastic model cellular heterogeneity for each timed outcome is described with random variables (RVs). Each RV must be allocated a parametric distribution that, at present, can only be determined by experiment. Distributions are required for each variable, such as: “time to activation”; “division time”; “time to destiny” and “time to death”. The appropriate distribution for time to first division and time between subsequent divisions is known for B and T cells and is right-skewed and well approximated by a lognormal (logn) or gamma distribution [4, 23, 38]. Optimal distributions for “time to destiny” and “time to death” are not known and require further experiment. However, from experience right-skewed distributions, such as the lognormal, are suitable for time to die data [1, 17] and are used here to fit to such data in Figure 7.

In the absence of all the information needed to complete a fully representative stochastic model we adopt a hybrid model with deterministic activation and division times and stochastic independent times to destiny and times to die that assumes lognormal distributions for each. This hybrid model allows us to highlight the sensitivity of cell numbers generated over time to changes in time to destiny ($T_{dd}$) and time to death ($T_{dth}$). Note that for deterministic times to activation and subsequent divisions equation 1 counts the number of division rounds giving rise to a discontinuous stepwise function. We now replace this counter with a continuous division scale, and the final model is given by:

$$n(t) = \mathbb{E}\big(N(t)\big) = \Pr(t < T_{dth})$$

$$\times \left(\Pr(t < T_{dd}) n_0 2^{\mathrm{t}/\mathrm{t_s}} + \int_0^t \Pr(T_{dd} = \tau) n_0 2^{\tau/\mathrm{t_s}} d\tau\right) \qquad (3)$$

$$q(t) = \mathbb{E}\big(Q(t)\big) = \Pr(t < T_{dth}) \int_0^t \Pr(T_{dd} = \tau) n_0 2^{\tau/\mathrm{t_s}} d\tau \quad (4)$$

This is the model used in Fig. 7g and we also used this model to fit to data from Fig. 2, in Fig. 7f. Note in this equation *t* gives time from $t_a$. Total time to the first division then is given by $t_a + t_s$.

<u>Parameters used in Figure 7g and Supplementary Figure 6:</u>

Supplementary Figure 6:

Control (default) - $n_0$, 100 cells; $t_a$, 0 (ie. response following reprogramming is plotted); $t_s$, 10 h; $t_{dd}$, logn (median, 80 h (m, 4.38); s, 0.25); $t_{dth}$, logn (median, 100 h (m, 4.60); s, 0.30).

To alter programming by 20%, median values were changed. $t_{dd}$ to 96 h, $t_{dth}$ to 120 h.

Fig. 7g:

Data normalized to 100 at first time point (41 h) to adjust for differences in starting numbers due to variable infection rates.

All data - $n_0$ = 50; $t_a$, 28 h; $t_s$, 9.3 h;

Vector WT - $t_{dd}$, logn (m, 3.76; s, 0.27) = *a*; $t_{dth}$, logn (m, 3.99; s, 0.40) = *b*.

Myc WT - $t_{dd}$ logn (m, 4.28; s, 0.30) = *c*; $t_{dth}$, *b*

Vector Bcl2-Tg - $t_{dd}$, *a;* $t_{dth}$, logn (m, 4.94; s, 0.50) = *d*

Myc Bcl2-Tg - $t_{dd}$, *c*; $t_{dth}$, *d*.


37. Gett, A.V. & Hodgkin, P.D. A cellular calculus for signal integration by T cells. *Nat Immunol* **1**, 239-244 (2000).

38. Dowling, M.R. *et al.* Stretched cell cycle model for proliferating lymphocytes. *Proceedings of the National Academy of Sciences* **111**, 6377-6382 (2014).